doi:10.1017/S1431927614009477
Microsc. Microanal. 20 (Suppl 3), 2014

In Situ Biasing TEM Characterization of Resistive Switching Phenomena in TiO_2-based RRAM

Jonghan Kwon[1], Abhishek A. Sharma[2], James A. Bain[2], Yoosuf N. Picard[1], Marek Skowronski[1]

1. Dept. of Materials Sci. and Eng., Carnegie Mellon University, Pittsburgh, PA 15213, USA
2. Dept. of Electrical and Computer Eng., Carnegie Mellon University, Pittsburgh, PA 15213, USA

Oxygen vacancy motion and agglomeration into Magnéli phases are often associated with resistive switching in TiO_2 [1-2]. However, the defect distribution and changes of device resistance are still poorly linked and require direct analysis. Extensive *ex situ* analysis has lead to proposed switching mechanisms that invoke defect formation/motion, but direct observation of defect evolution is still lacking. Here, we report direct observation of Wadsley defect formation and evolution in relation to Magnéli phases and resistive switching using *in situ* electrical testing of single-crystal TiO_2-based devices inside the transmission electron microscope (TEM). This enables us to monitor structural transformations that accompany resistive switching.

Metal-Insulator-Metal (MIM) devices consist of W/TiO_2/TiN layers fabricated by sputtering TiN (70 nm) on oxygen vacancy-doped single-crystals of rutile TiO_2 (001) substrates, extracting ~1.5 × 3 μm specimens and attaching to W scanning tunneling microscopy (STM) probes, followed by electron-beam induced W deposition inside a dual-beam focused ion beam (FIB) system. Subsequently, the specimens were thinned down to ~100 nm thickness and polished using 5keV Ga+ ions in order to reduce the FIB-induced surface damage. The *in situ* biasing TEM analyses were performed in an FEI Tecnai F20 with a Nanofactory® *in situ* biasing holder (single-tilt). An Agilent Semiconductor Parameter Analyzer was used to apply DC sweeps. A piezo-driven nano-manipulated W probe equipped within the *in situ* biasing holder made an electrical contact to the devices as shown in Fig. 1. A 12 kΩ external series resistor was connected to the circuit to suppress excessive transient current due to parasitic capacitance discharge while applying voltage. Figure 2 shows a bright-field (BF) TEM image of the as fabricated single-crystal device.

TEM analyses coordinated with electrical biasing show that electroforming causes electrical resistivity decreases while also inducing Magnéli phase formation. Magnéli phase regions starts at the W/TiO_2 interface and extends towards the TiO_2/TiN interface, covering nearly the entire sample (Fig. 3(a)). A ~50 nm Magnéli phase-free zone observed at the TiO_2/TiN interface is shown as an inset in Fig. 3(a). Selected area diffraction patterns (SADPs) near the [100] zone axis before and after Magnéli phase formation (Fig. 3 (b) and (c)) reveal satellite reflections along <011> directions consistent with {011} shear planes. The satellite reflections indicate the presence of oxygen-deficient Magnéli phases, known to have metallic conductivity between 30-1000 /W-cm [3]. After electroforming, the device exhibits very stable resistive switching with the current-voltage behavior shown in Fig. 4. Device resistance is correlated with the extent of Wadsley defects (missing planes of oxygen in the rutile structure). The oxygen vacancy accumulation in the Magnéli phase-free zone corresponds to extension of Wadsley defects into the zone as the device undergoes SET processes (Fig. 5(a, c)). The defects retract during RESET processes (Fig. 5(b)), thus ascertaining the physical locality of oxygen vacancies during switching. These ts individually or that the electrical conductivity of a defect-free insulating barrier is actively augmented by oxygen vacancy motion near the TiN bottom electrode. Nevertheless, the

filamentary resistive switching mechanism is now further validated at the micron-length scales by this study.

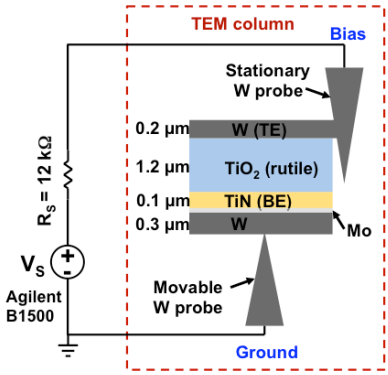

Fig. 1. Schematic showing *in situ* biasing TEM setup. TE and BE refer to top and bottom electrodes, respectively.

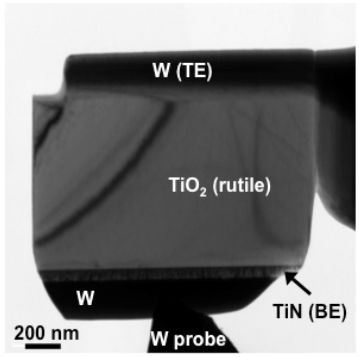

Fig. 2. BF TEM image of as fabricated $W/TiO_2/TiN$ device.

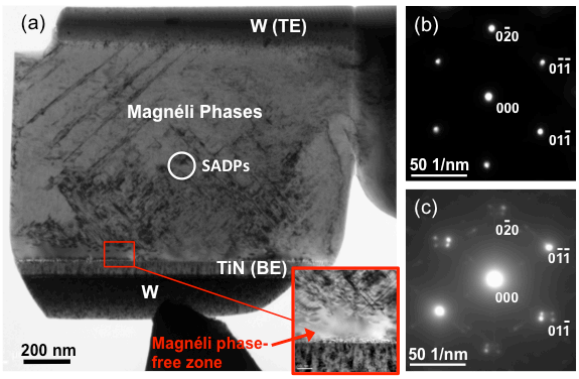

Fig. 3. BF TEM image showing Magnéli phases after electroforming (a), SADPs of specimen (b) before and (c) after Magnéli phase formation.

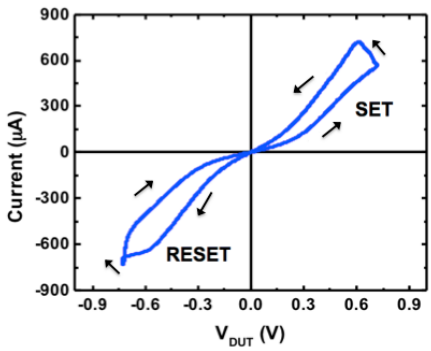

Fig. 4. Current-voltage curve showing hysteretic resistive switching behavior.

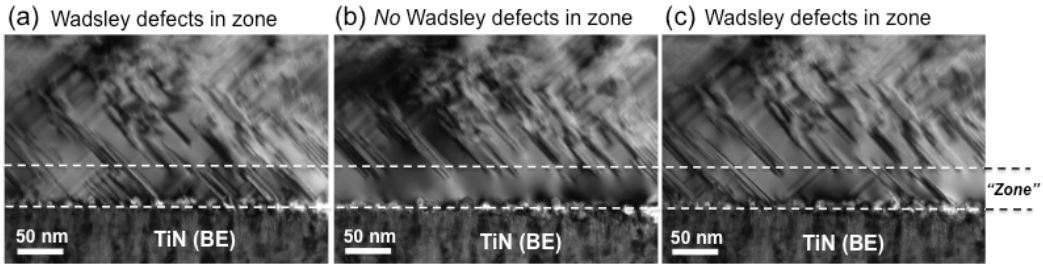

Fig 5. BF TEM images during a series of switching events. (a, c) BF TEM images showing extension of Wadsley defects after SET processes, (b) retraction of Wadsley defects after RESET process with in the Magnéli phasefree zone.

Reference

[1] D. Jeong et al., J. Appl. Phys., 104, 123716 (2008)
[2] K.M. Kim et al., Nanotechnology, 22, 254002 (2011)
[3] K. Szot et al., Nanotechnology, 22, 254001 (2011)

https://doi.org/10.1017/S1431927614009477 Published online by Cambridge University Press